

Micromechanical Electrostatic K-Band Switches

Student Paper

Sergio Pacheco, Clark T. Nguyen,[†] and Linda P. B. Katehi

The Radiation Laboratory
[†]Center for Integrated Sensors and Circuits
Electrical Engineering and Computer Science Department
University of Michigan, Ann Arbor, MI 48109-2122, USA

Abstract — Two novel designs of micromechanical capacitive switches using serpentine and cantilever springs for low actuation voltage applications are reported. Both designs also incorporate an electrode situated above the switching structure in order to provide system stability. DC measurements indicate pull-in voltages of 14 and 16 V, with RF isolation of better than -30 dB up to 40 GHz.

I. INTRODUCTION

Over the past several years, developments in microelectromechanical systems (MEMS) have promoted exciting advancements in the field of microwave switching. Bulk and surface micromachining have enabled the fabrication of intricate three-dimensional structures with great reliability. Micromechanical switches were first demonstrated by Petersen [1] as cantilever beams used in low-frequency applications. In 1991, Larson *et al.* described rotary micromechanical switches with good performance at frequencies up to 40 GHz [2]. However, these structures required high actuation voltages.

Recently, miniature micromechanical microwave switches with actuation voltages between 28 and 50 volts have been developed [3-5]. Such switches rival the performance of conventional solid-state switching devices such as p-i-n diodes and GaAs FETs.

However, for applications in wireless and/or space/airborne systems much lower voltages are necessary. In addition, the switches must be small in size and have low insertion loss. The electrostatic micromechanical switch described here achieves low switching voltage in a compact design by means of capacitive switching.

II. SWITCH DESIGN

Two micromechanical switch designs have been specifically developed for low actuation or pull-in voltage. Fig-

ures 1 and 2 show micrographs for the serpentine and cantilever beam switch designs respectively.

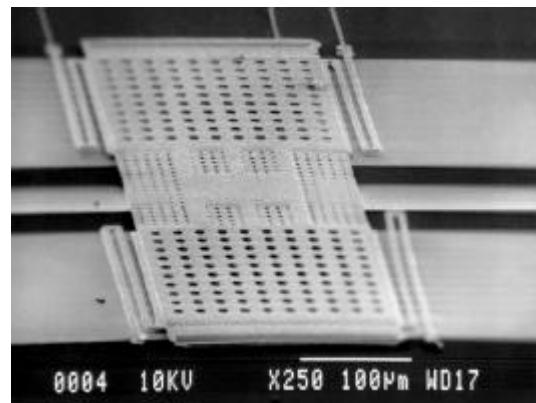


Figure 1. Micromechanical Switch with Serpentine Springs

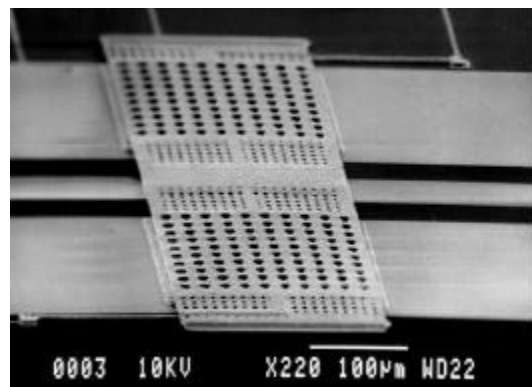


Figure 2. Micromechanical Switch with Cantilever Springs

The designs are basically identical except for the configuration of the springs attached to the switch. The serpen-

tine springs contain two meanders 220 μm in length while the cantilever beams are 250 μm in length. Both springs are 4 μm wide and the switches are 4.2 μm above a finite-ground coplanar waveguide (FGCPW) line [6]. The actuation pads are 220 μm x 220 μm in dimension and the entire switch structure is composed of 2 μm of electroplated gold.

The pull-in voltage for the switch can be determined from:

$$V_{pi} = \sqrt{\frac{8Kg_0^3}{27\epsilon_0 A}}$$

where K is the spring constant, g_0 is the height of the switch above the bottom electrode when there is no applied electrostatic field, ϵ_0 is the permittivity of air and A is the area of the actuation pad. Since the switches are placed above FGCPW lines, the necessary return loss associated with the RF signal restricts the value of the gap. The actuation pad area is also constrained in order to keep the structure compact. Therefore, the serpentine and cantilever springs have been designed to achieve a low spring constant. The choice of gold as the material is also important due to its low Young's Modulus ($E = 80$ GPa). Square holes 10 μm on a side are included in the actuation pad design in order to decrease the squeeze film damping of air and thus increase the Q of the system. The effect of the holes on the capacitance between electrodes has been studied and found to be minimal due to fringing fields [7]. Table 1 shows the mechanical parameters for each of the designs.

Table 1: Mechanical Parameters for Micromechanical Switches

	Serpentine	Cantilever
Mass	1.48×10^{-9} kg	1.49×10^{-9} kg
Spring Constant	0.478 N/m	0.654 N/m
Damping Coefficient	6.76×10^{-7} N/m/s	6.76×10^{-7} N/m/s
Actuation Voltage	4.95 V	5.79 V
Resonant Frequency	17.97 kHz	20.95 kHz

The extremely low values for K, however, mean that the switches become too compliant and can move in an environment of high pressure and acceleration gradients. To circumvent this problem, an electrode was placed above the switch in a single-pole, double-throw configuration (see Figure 3f). The top electrode is 200 μm wide, 650 μm long and 2 μm thick of electroplated gold. A constant applied voltage maintains the switch clamped to the top electrode preventing any undesired movement of the

switch. At the time of switching, the voltage between top electrode and switch is removed and the necessary pull-in voltage is applied between the ground plane of the FGCPW line and the switch. Once the switch clamps down, the high capacitance present at the center conductor provides a virtual short at RF.

III. FABRICATION PROCESS

A five mask batch process is used to fabricate the micro-mechanical switches. Figure 3 shows the fabrication process flowchart.

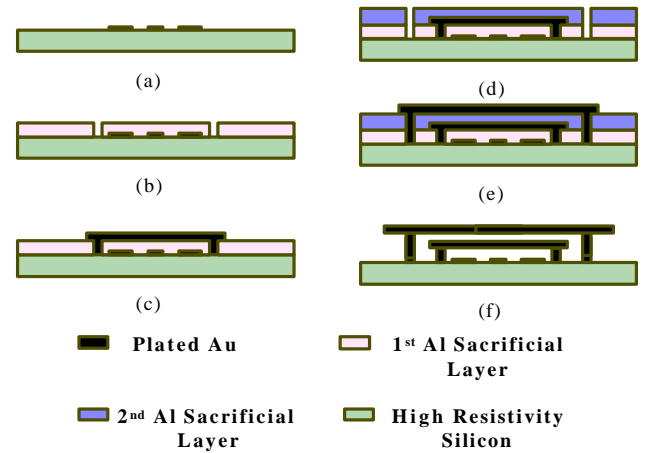


Figure 3. Fabrication Process Flowchart

(a) 500/5000 \AA of Cr/Al is deposited as a planarization layer. An image reversal lithography is performed to define the FGCPW lines, the Cr/Al is selectively etched, 500/5000 \AA of Ti/Au is blanket evaporated and removed from the field areas via a liftoff. (b) the first sacrificial layer of Al (3 μm) is deposited through sputtering and the posts for the switches are defined. (c) 500/2000/500 \AA of Ti/Au/Ti seed layer is sputtered on top of the first Al sacrificial layer, the switches are defined and 2 μm of Au is electroplated. (d) the second sacrificial layer of Al (1 μm) is deposited through sputtering and the posts for the top electrode are defined. (e) 500/2000/500 \AA of Ti/Au/Ti seed layer is sputtered on top of the second Al sacrificial layer, the top electrodes are defined and 2 μm of Au is electroplated. (f) both Al sacrificial layers are removed using hot Transene Type A Aluminum etchant and the Cr layer is removed in CR-14 Chrome etchant. The structures are rinsed in deionized water and isopropyl alcohol and then transferred to a Samdri-780A chamber for the supercritical CO_2 release of the structures. Finally, the switches are conformally coated with 500 \AA of parylene in a PDS 2010 dif-fuser in order to avoid stiction problems.

Planarization of the circuit level is an important aspect of the fabrication. It is vital that the switch structure is free of bends and/or cracks which can promote stress, fatigue and eventually rupture of the springs. The planarization of the top electrode was not a concern since it serves the sole purpose of immobilizing the switch.

IV. MEASUREMENTS

The actuation voltage measurements were performed using a HP 4275A Multi-Frequency LCR meter with an internal bias option. The capacitance versus voltage curves for the two designs are shown in Figures 4 and 5. The higher than expected actuation voltages (14 V and 16 V respectively) can be traced to the compressive internal stress of the gold material which hampers the switch's movement. This stress is evident by the bowing of the spring structures upon release. Even though a quantitative measure of this deflection has not been performed, it is evident from this study that slow gold electrodeposition can considerably reduce internal stress and consequently decrease the actuation voltage.

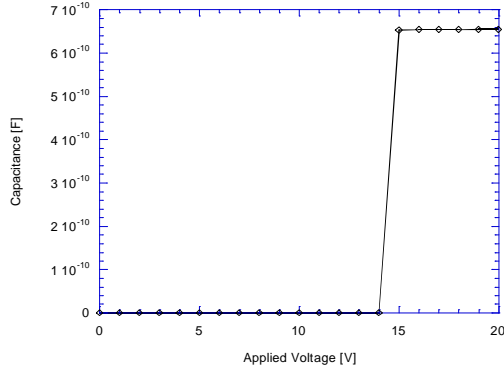


Figure 4. Pull-in Voltage for Switch with Serpentine Springs

The ratio of on/off capacitances is quite high, indicating that the parylene coating underneath the switch location is very thin. The on capacitance in both cases is in the nF range insuring that the FGCPW line does short out.

The RF response of the system has been measured using a GGB C-4 SOLT calibration standard with an 8510C Network Analyzer and Alessi Probe Station and GGB Pico-probe 150 μm pitch coplanar probes. Figure 6 is a plot of response of a 2 mm FGCPW line without a switch.

Figure 7 shows the S-parameters for a serpentine spring switch in the off position. By comparison between the insertion loss of a thru line (Figure 6) and that of the switch

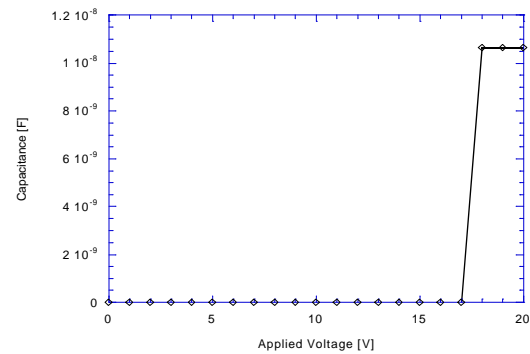


Figure 5. Pull-in Voltage for Switch with Cantilever Springs

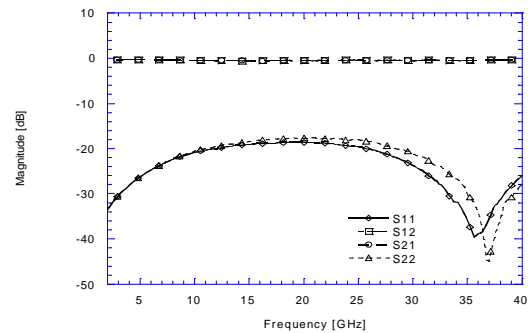


Figure 6. Measured S-Parameters for Thru Line

circuit (Figure 7), we can conclude that the insertion loss of the switch is less than 0.2 dB at 20 GHz.

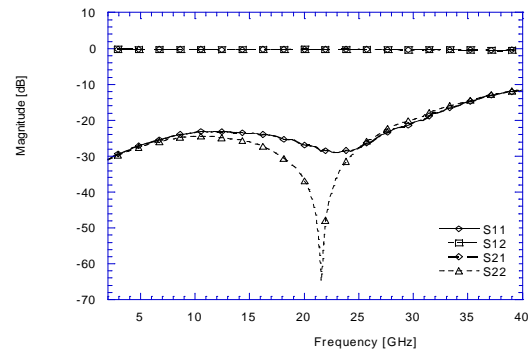


Figure 7. Measured S-Parameters for Serpentine Switch Off

The RF characteristics with the switch on is shown in Figure 8 and demonstrates an isolation of approximately -30 dB throughout most of the band.

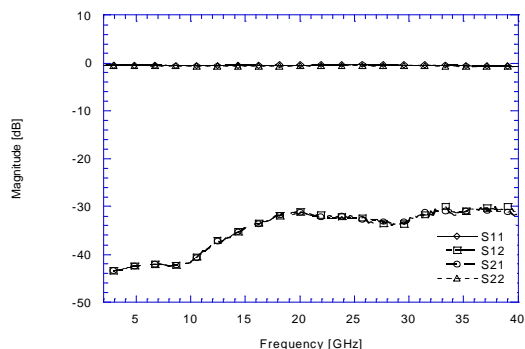


Figure 8. Measured S-Parameters for Serpentine Switch On

Figures 9 and 10 are the response for the cantilever spring design for the off and on case respectively. Again, it shows a return loss of better than -20 dB up to 30 GHz and an isolation of over -30 dB up to 40 GHz.

Variations of the two designs presented here are underway to improve the return loss of the device. These studies include new top electrode configurations to minimize coupling to the FGCPW line but without compromising stability. Also, a more detailed investigation of the internal stress of gold will be conducted.

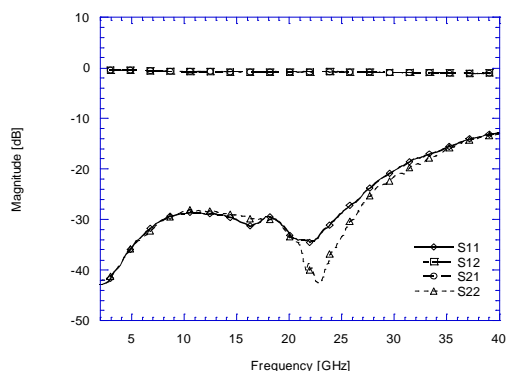


Figure 9. Measured S-Parameters for Cantilever Switch Off

V. CONCLUSIONS

Two micromechanical microwave switch designs for low voltage applications have been demonstrated. Low

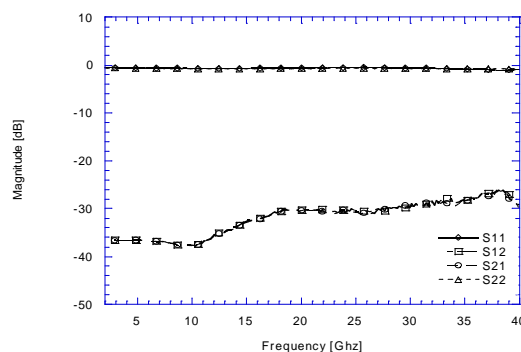


Figure 10. Measured S-Parameters for Cantilever Switch On

pull-in voltages were achieved by designing serpentine and cantilever beams attached to the switching structure with extremely low spring constant. Furthermore, the stability of the device was improved by the addition of a top electrode.

ACKNOWLEDGMENTS

This work has been supported by the MURI/ARO on Low Power Electronics Design.

REFERENCES

- [1] K. E. Petersen, "Micromechanical Membrane Switches on Silicon," *IBM J. Res. Develop.*, vol. 23, no. 4, pp. 376-385, July 1971.
- [2] L. E. Larson, R. H. Hackett, M. A. Melendes, and R. F. Lohr, "Micromachined Microwave Actuator (MIMAC) Technology - A New Tuning Approach for Microwave Integrated Circuits," *IEEE Microwave and Millimeter-Wave Monolithic Circuit Symposium*, pp. 27-30, 1991.
- [3] C. Goldsmith, T. H. Lin, B. Powers, W. R. Wu, and B. Norvell, "Micromechanical Membrane Switches for Microwave Applications," *IEEE MTT-S Digest*, pp. 91-94, 1995.
- [4] J. J. Yao and M. F. Chang, "A Surface Micromachined Miniature Switch for Telecommunications Applications with Signal Frequencies From DC up to 4 GHz," *The 8th International Conference on Solid-State Sensors and Actuators and Eurosensors IX*, pp. 384-387, 1995.
- [5] C. Goldsmith, J. Randall, S. Eshelman, and T. H. Lin, "Characteristics of Micromachined Switches at Microwave Frequencies," *IEEE MTT-S Digest*, pp. 1141-1144, 1996.
- [6] F. Brauchler, S. Robertson, J. East, and L. P. B. Katehi, "W-Band Finite Ground Coplanar (FGC) Line Circuit Elements," *IEEE MTT-S Digest*, pp. 1845-1848, 1996.
- [7] G. K. Fedder, "Simulation of Microelectromechanical Systems," *Doctor of Philosophy Dissertation*, University of California at Berkeley, 1994.